Template Synthesis of Macrocyclic Dinuclear Cu^{II} Complexes and Conversion into Mononuclear Complexes by Site-Selective Copper Elimination

Akiko Hori, Masami Yonemura, Masaaki Ohba, and Hisashi Ōkawa*

Department of Chemistry, Faculty of Science, Kyushu University, Hakozaki 6-10-1, Higashiku, Fukuoka 812-8581

(Received October 10, 2000)

The acyclic dinucleating ligand, *N*,*N*′-dimethyl-*N*,*N*′-trimethylenedi-(3-formyl-2-hydroxy-5-methylbenzylamine) (H_2L), has been prepared. It combines two Cu^{II} ions with its $N(amine)_2O_2$ and O_4 metal-binding sites to form a dinuclear complex $[Cu_2(L)](ClO_4)_2$. The [1:1] condensation of $[Cu_2(L)](ClO_4)_2$ with an aliphatic or aromatic diamine has provided macrocyclic dinuclear Cu^{II} complexes $[Cu_2(L^i)](ClO_4)_2$ ($L^i = L^1$ for the diamine = ethylenediamine, L^2 for trimethylenediamine, L^3 for tetramethylenediamine, L^4 for *o*-phenylenediamine and L^5 for 1,8-diaminonaphthalene). X-ray crystallographic studies for $[Cu_2(L^1)(H_2O)](ClO_4)_2$·MeCN and $[Cu_2(L^5)](ClO_4)_2$·2MeOH demonstrate a macrocyclic dinuclear core structure with the two Cu^{II} ions in the $N(amine)_2O_2$ and $N(imine)_2O_2$ sites, in the Cu–Cu separation of ca. 3.0 Å. The dinuclear complexes are studied in magnetic, electronic spectral and electrochemical properties. The treatment of the dinuclear complexes with Na_2S in acetonitrile resulted in the elimination of one Cu to afford the mononuclear complexes $[Cu(L^i)]$·$x$$NaClO_4$. The X-ray crystallography for $[Cu(L^2)]$, $[Cu(L^3)]$·$NaClO_4$ and $[Cu(L^4)]$ has demonstrated that the Cu in the $N(amine)_2O_2$ site is selectively eliminated. In the latter complex, the Na^I ion is accommodated in the aminic site.

The design of dinucleating compartmental ligands capable of binding two metal ions in close proximity is important for providing functional bimetallic molecules and for modeling bimetallic biosites.[1,2] Phenol-based macrocyclic ligands of the type in Scheme 1, having dissimilar $N(amine)_2O_2$ and $N(imine)_2O_2$ metal-binding sites sharing the bridging phenolic oxygens, have been used for the study of heterodinuclear metal complexes.[2–6] The macrocyclic ligands are synthesized by two steps; (i) the preparation of an acyclic proligand possessing $N(amine)_2O_2$ and $O(formyl)_2O_2$ metal-binding sites and (ii) the 1:1 condensation of the proligand with a diamine by a template reaction. The key step in this synthesis is the preparation of an appropriate proligand. Previously we reported two macrocyclic ligands of this type (X = Br, R = CH_3, L^a = ethylene, L^b = ethylene or trimethylene),[4,5] where the proligand *N*,*N*′-dimethyl-*N*,*N*′-ethylenedi(5-bromo-3-formyl-2-hydroxybenzylamine) was easily prepared by the Mannich reaction between 5-bromosalicylaldehyde and *N*,*N*′-dimethylethylenediamine. This synthetic method seemed to be applicable to analogous proligands with different lateral chains between the amine nitrogens. In our attempt to prepare the proligand, *N*,*N*′-dimethyl-*N*,*N*′-trimethylenedi(5-bromo-3-formyl-2-hydroxybenzylamine), however, the Mannich reaction between 5-bromosalicylaldehyde and *N*,*N*′-dimethyl-1,3-trimethylenediamine resulted in the recovery of the starting materials in spite of our many efforts. Thus, one needs to develop a new synthetic method of proligands for the macrocyclic ligands of the type in Scheme 1.

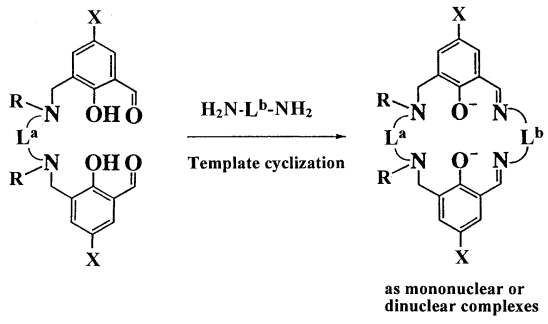

Scheme 1. General synthetic scheme of macrocyclic complexes.

This work relates to a new preparation of an acyclic proligand, *N*,*N*′-dimethyl-*N*,*N*′-trimethylenedi(5-methyl-3-formyl-2-hydroxybenzylamine) (abbreviated as H_2L), by the reaction between 3-chloromethyl-5-methylsalicylaldehyde and *N*,*N*′-dimethyl-1,3-propanediamine, and the template cyclization with an aliphatic or aromatic diamine to afford macrocyclic dinuclear Cu^{II} complexes $[Cu_2(L^i)](ClO_4)_2$ (Scheme 2). The abbreviations of the macrocyclic ligands are as follows: $L^i = L^1$ for Z = ethylene, L^2 for trimethylene, L^3 for tetramethylene, L^4 for *o*-phenylene and L^5 for 1,8-naphthalene. The structures of $[Cu_2(L^1)(H_2O)](ClO_4)_2$·MeCN and $[Cu_2(L^5)](ClO_4)_2$·2MeOH are determined, and physicochemical properties of $[Cu_2(L^i)](ClO_4)_2$ are investigated. The treatment of $[Cu_2(L^i)](ClO_4)_2$ with Na_2S in acetonitrile gave $[Cu(L^i)]$·x$NaClO_4$. The site-selective elimination of the Cu in the $N(amine)_2O_2$ site is reported.

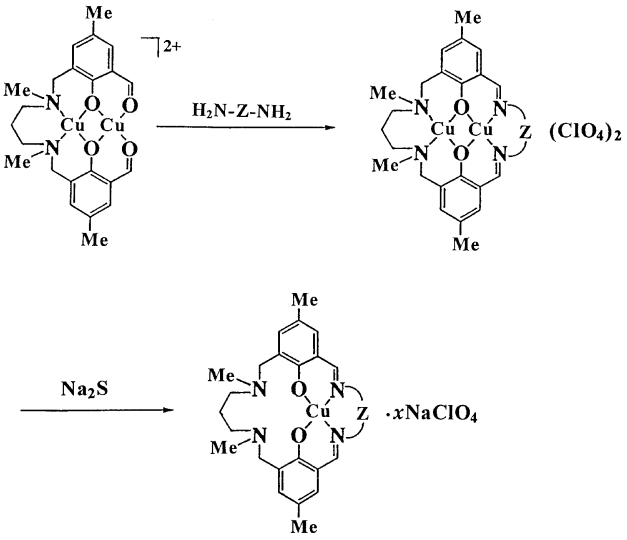

Scheme 2. Synthetic scheme for L^1–L^5 as dinuclear Cu^{II} complexes and conversion into mononuclear complexes.

Experimental

Measurements. Elemental analyses of C, H and N were obtained from the Service Center of Elemental Analysis at Kyushu University. Analyses of Cu were obtained using a Shimadzu AA-660 atomic absorption/flame emission spectrophotometer. Infrared spectra were recorded on a Perkin Elmer BX FT-IR system using KBr disks. Electronic spectra in *N*,*N*-dimethylformamide (dmf) were recorded on a Shimadzu UV-3100PC spectrometer. Magnetic susceptibilities were measured on a Faraday balance in the temperature range of 78–300 K. The apparatus was calibrated using $[Ni(en)_3]S_2O_3$;[7] diamagnetic corrections for the constituting atoms were performed using Pascal's constants.[8] Cyclic voltammograms were recorded on a BAS CV-50W electrochemical analyzer in dmf or dichloromethane containing tetrabutylammonium perchlorate (TBAP) as the supporting electrolyte (**Caution!** TBAP is explosive and should be handled with great care). A three-electrode cell was used which was equipped with a glassy carbon as the working electrode, a platinum coil as the counter electrode, and a Ag/Ag^+ (TBAP/acetonitrile) electrode as the reference.

Preparation. 3-Chloromethyl-5-methylsalicylaldehyde was prepared by the literature methods.[9,10] Other chemicals were purchased from commercial sources and used without further purification.

***N*,*N*′-Dimethyl-*N*,*N*′-trimethylenedi(3-formyl-2-hydroxy-5-methylbenzylamine) (H_2L).** A solution of *N*,*N*′-dimethyl-1,3-propanediamine (1.38 g, 13.5 mmol) and triethylamine (2.74 g, 27 mmol) in tetrahydrofuran (20 cm^3) was dropwise added to a stirred solution of 3-chloromethyl-5-methylsalicylaldehyde (5.0 g, 27 mmol) in tetrahydrofuran (20 cm^3), and the mixture was refluxed for 3 hours. The reaction mixture was diluted with water (50 cm^3) and shaken with three 50 cm^3 portions of chloroform. The extracts were combined, washed with water, and dried over $MgSO_4$. Crude H_2L was obtained as an oily substance when the solvent was evaporated to dryness. It was used for the preparation of the following complex without further purification.

$[Cu_2(L)](ClO_4)_2$. H_2L (4.18 g, 10.0 mmol) and copper(II) acetate monohydrate (2.12 g, 10.4 mmol) were dissolved in methanol (50 cm^3), and the solution was stirred for 20 minutes. To this was added a solution of copper(II) perchlorate hexahydrate (3.84 g, 10.4 mmol) in methanol (20 cm^3), and the mixture was stirred at room temperature for 2 hours to give green microcrystals. Yield: 6.76 g (90%). Found: C, 38.09; H, 4.21; N, 3.79; Cu, 17.9%. Calcd for $C_{23}H_{28}Cl_2Cu_2N_2O_{12}$: C, 38.24; H, 3.91; N, 3.88; Cu, 17.6%. μ_{eff} per Cu: 1.03 μ_B at 290 K. Selected IR data (ν/cm^{-1}) using KBr disk: 1612, 1561, 1117, 1082, 814, 621. UV-vis λ/nm (ε/M^{-1} cm^{-1}) in dmf: 374 (7900), 668 (180) (1 M = 1 mol dm^{-3}).

Recrystallization from dmf formed $[Cu_2(L)(dmf)_2](ClO_4)_2$ as green prisms suitable for X-ray crystallography.

$[Cu_2(L^1)](ClO_4)_2$ (1). To a solution of $[Cu_2(L)](ClO_4)_2$ (500 mg, 0.69 mmol) in acetonitrile (100 cm^3) was added ethylenediamine (41 mg, 0.69 mmol), and the mixture was stirred for 10 hours and concentrated to 20 cm^3 to give greenish brown microcrystals. Yield: 390 mg (76%). Found: C, 39.84; H, 4.48; N, 7.87; Cu, 16.7%. Calcd for $C_{25}H_{32}Cl_2Cu_2N_4O_{10}$: C, 40.22; H, 4.32; N, 7.50; Cu, 17.0%. μ_{eff} per Cu: 0.85 μ_B at 290 K. Selected IR data (ν/cm^{-1}) using KBr disk: 2926, 1642, 1570, 1463, 1110, 1087, 804, 622. UV-vis λ/nm (ε/M^{-1} cm^{-1}) in dmf: 348 (9100), ca. 470(sh), 654 (145).

Recrystallization from acetonitrile formed **1**·H_2O·MeCN as good crystals suitable for X-ray crystallography.

$[Cu_2(L^2)](ClO_4)_2$ (2). To a solution of $[Cu_2(L)](ClO_4)_2$ (500 mg, 0.69 mmol) in acetonitrile (100 cm^3) was added trimethylenediamine (51 mg, 0.69 mmol), and the mixture was stirred for 10 hours to result in the precipitation of the mononuclear complex $[Cu(L^2)]$ (**2′**, see below) as brown crystals (127 mg). The solution separated from **2′** was concentrated to 20 cm^3 and allowed to stand overnight to give the dinuclear complex **2** as green microcrystals. Yield: 240 mg (46%). Found: C, 40.84; H, 4.54; N, 7.36; Cu, 16.5%. Calcd for $C_{26}H_{34}Cl_2Cu_2N_4O_{10}$: C, 41.06; H, 4.51; N, 7.37; Cu, 16.7%. μ_{eff} per Cu: 1.05 μ_B at 290 K. Selected IR data (ν/cm^{-1}) using KBr disk: 2927, 1636, 1575, 1468, 1098, 812, 620. UV-vis λ/nm (ε/M^{-1} cm^{-1}) in dmf: 346 (11200), 64 (190).

$[Cu_2(L^3)](ClO_4)_2$ (3). This was obtained as dark green crystals by the reaction of $[Cu_2(L)](ClO_4)_2$ with tetramethylenediamine. Yield: 60%. Found: 41.79; H, 4.79; N, 7.30; Cu, 16.6%. Calcd for $C_{27}H_{36}Cl_2Cu_2N_4O_{10}$: C, 41.87; H, 4.68; N, 7.23; Cu, 16.4%. μ_{eff} per Cu: 0.72 μ_B at 290 K. Selected IR data (ν/cm^{-1}) using KBr disk: 2944, 1626, 1573, 1467, 1093, 810, 601. UV-vis (λ/nm (ε/M^{-1} cm^{-1}) in dmf: 348 (11900), 646 (195), ca. 730 (100).

$[Cu_2(L^4)](ClO_4)_2$ (4). This was obtained as brown microcrystals by the reaction of $[Cu_2(L)](ClO_4)_2$ with *o*-phenylenediamine. Yield: 73%. Found: 43.62; H, 4.21; N, 7.27; Cu, 15.9%. Calcd for $C_{29}H_{32}Cl_2Cu_2N_4O_{10}$: C, 43.84; H, 4.06; N, 7.05; Cu, 16.0%. μ_{eff} per Cu: 0.77 μ_B at 290 K. Selected IR data (ν/cm^{-1}) using KBr disk: 3010, 1614, 1561, 1460, 1087, 807, 622. UV-vis λ/nm (ε/M^{-1} cm^{-1}) in dmf: 346 (10300), 375 (6900), 402 (6700), 560 (180), 656 (170).

$[Cu_2(L^5)](ClO_4)_2$ (5). This was obtained as brown microcrystals by the reaction of $[Cu_2(L)](ClO_4)_2$ with 1,8-diaminonaphthalene. Yield: 83%. Found: 46.45; H, 4.26; N, 6.46; Cu, 14.8%. Calcd for $C_{33}H_{33}Cl_2Cu_2N_4O_{10}$: C, 46.93; H, 3.94; N, 6.64; Cu, 15.1%. μ_{eff} per Cu: 0.77 μ_B at 290 K. Selected IR data (ν/cm^{-1}) using KBr disk: 1622, 1594, 1572, 1553, 1236, 1093, 829, 627. UV-vis λ/nm (ε/M^{-1} cm^{-1}) in dmf: 392 (10200), 656 (170), 680 (140).

It was recrystallized from a dmf-methanol mixture as **5**·2MeOH suitable for X-ray crystallography.

Conversion of Dinuclear Complexes (1–5) into Mononuclear Complexes (1′–5′). Each of **1**–**5** (0.1 mmol) and Na_2S·$9H_2O$ (0.1 mmol) were added to acetonitrile (30 cm^3), and the mixture was

stirred at ambient temperature for 1 hour. The resulting CuS was separated by filtration, and the filtrate was diffused with 2-propanol to give a crystalline product.

[Cu(L^1)]·0.8NaClO$_4$ (1′·0.8NaClO$_4$). Brown-purple microcrystalline powder. Yield: 58%. Found: 51.64; H, 5.56; N, 9.52; Cu, 10.9%. Calcd for $C_{25}H_{32}CuN_4O_2$·0.8NaClO$_4$ C, 51.59; H, 5.54; N, 9.63; Cu, 10.9%. μ_{eff} per Cu: 1.84 μ_B at 290 K. Selected IR data (ν/cm^{-1}) using KBr disk: 2786, 1627, 1571, 1097, 620.

[Cu(L^2)] (2′). Brown microcrystals. Yield: 75%. Found: C, 62.78; H, 6.59; N, 11.15; Cu, 12.6%. Calcd for $C_{26}H_{34}CuN_4O_2$: C, 62.69; H, 6.88; N, 11.25; Cu, 12.8%. μ_{eff} per Cu: 1.92 μ_B at 290 K. Selected IR data (ν/cm^{-1}) using KBr disk: 2940, 2788, 2757, 1619, 1601, 1543, 1448. UV-vis λ/nm (ε/M^{-1} cm^{-1}) in dmf: 388 (11100), 607 (316).

It was recrystallized from a dmf-methanol mixture as single crystals suitable for X-ray crystallography.

[Cu(L^3)]·NaClO$_4$ (3′·NaClO$_4$). Dark green microcrystals. Yield: 85%. Found: 51.49; H, 5.71; N, 9.02; Cu, 10.2%. Calcd for $C_{27}H_{36}ClCuN_4NaO_6$: C, 51.10; H, 5.72; N, 8.83; Cu, 10.0%. FABMS: m/z 534.4 for {NaCu(L^3)}$^+$. μ_{eff} per Cu: 1.93 μ_B at 290 K. Selected IR data (ν/cm^{-1}) using KBr disk: 2926, 2798, 1623, 1601, 1095, 1063, 621. UV-vis λ/nm (ε/M^{-1} cm^{-1}) in dmf: 380 (9300), 600 (250).

[Cu(L^4)] (4′). Reddish brown microcrystals. Yield: 77%. Found: 65.18; H, 6.06; N, 10.52; Cu, 12.0%. Calcd for $C_{29}H_{32}CuN_4O_2$: C, 65.46; H, 6.06; N, 10.53; Cu, 11.9%. μ_{eff} per Cu: 1.85 μ_B at 300 K. Selected IR data (ν/cm^{-1}) using KBr disk: 2920, 2788, 1618, 1601. UV-vis λ/nm (ε/M^{-1} cm^{-1}) in dmf: 313 (27000), 446 (21600), 590 (410).

[Cu(L^5)]·2.1NaClO$_4$ (5′·2.1NaClO$_4$). Brown microcrystalline powder. Yield: 72%. Found: C, 47.07; H, 4.43; N, 6.79; Cu, 8.1%. Calcd for $C_{33}H_{34}CuN_4O_2$·2.1NaClO$_4$: C, 47.22; H, 4.08; N, 6.68; Cu, 7.6%. μ_{eff} per Cu: 1.93 μ_B at 300 K. Selected IR data (ν/cm^{-1}) using KBr disk: 1622, 1581, 1549, 1539, 1227, 1093, 762, 624. UV-vis λ/nm (ε/M^{-1} cm^{-1}) in dmf: 404 (28000).

X-Ray Crystallography. Crystallographic measurements for [Cu$_2$(L)(dmf)$_2$](ClO$_4$)$_2$, **5**·2MeOH, **2′**, **3′**·NaClO$_4$ and **4′** were made on a Rigaku AFC7R diffractometer using graphite-monochromated Mo$K\alpha$ radiation (λ = 0.71069 Å) and a 12 kW rotating anode generator. Data collections of **1**·H$_2$O·MeCN were made on a Rigaku AFC5S diffractometer. Cell constants and an orientation matrix for the data collection were obtained from 25 reflections and the ω-2θ scan technique was used for the intensity collections. Pertinent crystallographic parameters are summarized in Table 1.

The intensities of the representative reflections were monitored every 150 reflections and decay corrections were applied. An empirical absorption correction based on azimuthal scans of several reflections was applied. Reflection data were corrected for Lorentz and polarization effects.

The structures were solved by the direct method and expanded using the Fourier technique. Non-hydrogen atoms were refined anisotropically. Hydrogen atoms were included in structure factor calculations but were not refined. In the case of **5**·2MeOH, one of the perchlorate ions and the two MeOH molecules were refined isotropically because of positional disorder. The neutral atom scattering factors were taken from Cromer and Waber.[11] Anomalous dispersion effects were included in F_{calcd}; the values for $\Delta f'$ and $\Delta f''$ were those of Creagh and McAuley.[12] The values for the mass attenuation coefficients are those of Creagh and Hubbel.[13] All calculations were performed using the teXsan[14] crystallographic software of Molecular Structure Corporation.

Crystallographic data have been deposited at the CCDC, 12 Union Road, Cambridge CB2 1EZ, UK and copies can be obtained on request, free of charge, by quoting the publication citation and deposition numbers CCDC 154024–154027. The data are also deposited as Document No. 74021 at the Office of the Editor of Bull. Chem. Soc. Jpn.

Results and Discussion

Precursor Complex [Cu$_2$(L)](ClO$_4$)$_2$. Preparation. In our previous work the proligand *N*,*N*′-dimethyl-*N*,*N*′-ethylenedi(5-bromo-3-formyl-2-hydroxybenzylamine) formed a mononuclear Cu^{II} complex with the metal in the N(amine)$_2$O$_2$ site.[5a] The cyclization of the Cu complex with ethylenediamine or 1,3-trimethylenediamine afforded the macrocyclic Cu^{II} complexes, and a similar cyclization reaction in the presence of Pb^{II} afforded the macrocyclic Pb^{II}Cu^{II} complexes. Both the

Table 1. Crystal Parameters

	[Cu$_2$(L)(dmf)$_2$](ClO$_4$)	**1**·H$_2$O·MeCN	**5**·2MeOH	**2′**	**3′**·NaClO$_4$	**4′**
Formula	$C_{29}H_{42}N_4Cl_2Cu_2O_{14}$	$C_{27}H_{37}N_5Cl_2Cu_2O_{11}$	$C_{34}H_{38}N_4Cl_2Cu_2O_{11}$	$C_{26}H_{34}N_4CuO_2$	$C_{27}H_{36}N_4ClCuNaO_6$	$C_{29}H_{32}N_4CuO_2$
Formula weight	868.67	805.61	876.69	498.13	634.59	532.14
Crystal system	orthorhombic	triclinic	orthorhombic	monoclinic	monoclinic	monoclinic
Space group	$P2_12_12_1$(#19)	$P\bar{1}$(#2)	*Pbcn* (#60)	*C*2/*c* (#15)	$P2_1/c$(#14)	$P2_1/c$(#14)
a/Å	18.338(10)	10.682(2)	20.805(5)	19.885(5)	12.778(3)	8.371(3)
b/Å	20.407(7)	16.427(4)	23.863(8)	14.262(5)	13.100(4)	15.026(3)
c/Å	9.954(2)	10.082(2)	15.122(2)	9.451(4)	17.352(4)	19.854(2)
α/°	90	98.30(2)	90	90	90	90
β/°	90	104.56(1)	90	115.00(2)	97.198(2)	93.26(2)
γ/°	90	103.60(2)	90	90	90	90
V/Å^{-3}	3724(2)	1624.9(6)	7507(2)	2429(1)	2881(1)	2493(1)
Z value	4	2	4	8	4	4
Dc/g cm^{-3}	1.549	1.646	1.551	1.362	1.463	1.418
μ(Mo$K\alpha$)/cm^{-1}	13.54	15.39	13.39	9.29	9.13	9.11
No. observations ($I > 3.00\sigma(I)$)	2474	3346	3882	1720	4543	2984
R	0.048	0.042	0.066	0.041	0.049	0.043
R_W	0.056	0.038	0.090	0.046	0.075	0.043

macrocyclic Cu^{II} and $Pb^{II}Cu^{II}$ complexes could be used as precursors for the transition metal dinuclear $M^{II}Cu^{II}$ complexes.[5] In this work the new proligand *N*,*N*′-dimethyl-*N*,*N*′-trimethylenedi(5-methyl-3-formyl-2-hydroxybenzylamine) (H_2L) always formed dinuclear $[Cu_2(L)](ClO_4)_2$ even when syntheses were attempted in the stoichiometry of $H_2L/Cu^{II} = 1/1$. The cyclization of the proligand complex $[Cu_2(L)](ClO_4)_2$ with diamines formed the macrocyclic dinuclear Cu^{II} complexes (**1**–**5**) in a good or tolerable yield.

Crystal Structure. An ORTEP[15] view of the dmf adduct, $[Cu_2(L)(dmf)_2](ClO_4)_2$, is shown in Fig. 1 together with the numbering scheme. Selected bond distances and angles are summarized in Table 2.

The dinegative L^{2-} accommodates two Cu^{II} ions in its N_2O_2 and O_4 sites in the Cu–Cu separation of 3.040(2) Å. The geometry about Cu1 in the N_2O_2 site is a square-pyramid with a dmf oxygen at the axial site. The basal bond distances fall in the range of 1.991(6)–2.028(8) Å. The axial Cu1–O5(dmf) bond distance is 2.196(6) Å; this is elongated owing to the Jahn–Teller effect. The Cu1 is displaced by 0.160 Å from the basal N_2O_2 least-squares plane towards O5. The two methyl groups (C10 and C14) attached to the nitrogens are situated cis to each other with respect to the mean $\{CuN_2O_2\}$ plane. The trimethylene chain combining the two amino nitrogens assumes the usual chair conformation.

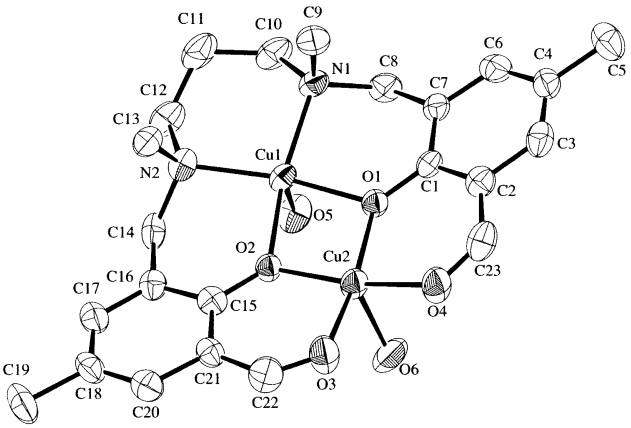

Fig. 1. An ORTEP view for $[Cu_2(L)(dmf)_2](ClO_4)_2$ with the atom numbering scheme.

Table 2. Selected Bond Distances and Angles for $[Cu_2(L)(dmf)_2](ClO_4)_2$

Bond Distances (Å)			
Cu(1)–O(1)	2.023(6)	Cu(1)–O(2)	1.991(6)
Cu(1)–O(5)	2.196(6)	Cu(1)–N(1)	2.024(8)
Cu(1)–N(2)	2.028(8)		
Cu(2)–O(1)	1.918(6)	Cu(2)–O(2)	1.932(6)
Cu(2)–O(3)	1.915(7)	Cu(2)–O(4)	1.909(7)
Cu(2)–O(6)	2.248(8)		
Cu(1)···Cu(2)	3.040(2)		
Bond Angles (°)			
O(1)–Cu(1)–O(2)	76.3(2)	O(1)–Cu(1)–O(5)	98.2(3)
O(1)–Cu(1)–N(1)	91.5(3)	O(1)–Cu(1)–N(2)	166.1(3)
O(2)–Cu(1)–O(5)	96.1(3)	O(2)–Cu(1)–N(1)	165.0(3)
O(2)–Cu(1)–N(2)	91.9(3)	O(5)–Cu(1)–N(1)	94.3(3)
O(5)–Cu(1)–N(2)	90.4(3)	N(1)–Cu(1)–N(2)	98.8(3)
O(1)–Cu(2)–O(2)	80.2(2)	O(1)–Cu(2)–O(3)	170.8(3)
O(1)–Cu(2)–O(4)	95.2(3)	O(1)–Cu(2)–O(6)	96.5(3)
O(2)–Cu(2)–O(3)	96.2(3)	O(2)–Cu(2)–O(4)	170.0(3)
O(2)–Cu(2)–O(6)	94.4(3)	O(3)–Cu(2)–O(4)	87.0(3)
O(3)–Cu(2)–O(6)	92.2(3)	O(4)–Cu(2)–O(6)	95.1(3)

The Cu2 in the O_4 site also has a square-pyramidal geometry together with a dmf oxygen (O6) at the axial site. The basal bond distances range from 1.909(7) to 1.932(6) Å. The axial Cu2–O6 bond distance is elongated (2.248(8) Å). The displacement of Cu2 from the basal least-squares plane towards O6 is 0.151 Å. The dmf molecule bound to Cu1 and that bound to Cu2 are situated cis with respect to the mean molecular plane.

The basal least-squares plane for Cu1 and that for Cu2 are bent at the O2–O3 edge with a dihedral angle of 21.03°. Furthermore, the molecule shows a bend at the Cu1–Cu2 edge, providing a saddle-like shape for the molecule. The dihedral angle defined by the two aromatic rings is 15.87°.

Properties. $[Cu_2(L)](ClO_4)_2$ shows the ν(C=O) vibration of the formyl group at 1610 cm^{-1}. The low frequency of the band is in harmony with the coordination of the formyl oxygen to the Cu.[16] The ν_3 mode of perchlorate group is split into two (1117 and 1082 cm^{-1}), suggesting the coordinative interaction of the perchlorate group.[17] The perchlorate groups must be bonded to the axial site of the two Cu^{II} ions, instead of the dmf ligands of $[Cu_2(L)(dmf)_2](ClO_4)_2$. In fact, $[Cu_2(L)(dmf)_2](ClO_4)_2$ shows a perchlorate ν_3 vibration at 1100 cm^{-1}. Electronic absorption spectrum of $[Cu_2(L)](ClO_4)_2$ in dmf has an intense band at 374 nm and a weak band at 668 nm. The former is assigned to an intraligand transition and the latter band to a superposition of the d–d transitions of the two Cu^{II} ions. The magnetic moment at room temperature is 1.03 μ_B per Cu, and the moment decreased with decreasing temperature to 0.29 μ_B at liquid nitrogen temperature due to an antiferromagnetic interaction between the two Cu^{II} ions. The magnetic simulation of this complex is discussed later, together with the dinuclear complexes **1**–**5**.

Macrocyclic Dinuclear Complexes. Crystal Structures. An ORTEP drawing of $[Cu_2(L^1)(H_2O)](ClO_4)_2$·MeCN (**1**·$H_2O$·MeCN) is shown in Fig. 2 together with the atom numbering scheme. Relevant bond distances and angles are summarized in Table 3.

The crystal is comprised of the macrocycle $(L^1)^{2-}$, two Cu ions and one water molecule: two perchlorate ions and one MeCN molecule are free from coordination and captured in the crystal lattice. The Cu1 in the $N(amine)_2O_2$ site (aminic site) has a square-pyramidal geometry together with the aqua oxygen O3 at the axial site. The basal bond distances range from 1.997(4) to 2.012(4) Å. The axial Cu1–O3 bond is short (2.304(4) Å). The deviation of the Cu from the basal least-squares plane toward O3 is 0.211 Å. The Cu2 in the $N(imine)_2O_2$ site (iminic site) has a planar geometry with the short bond distances of 1.898(4)–1.914(4) Å.

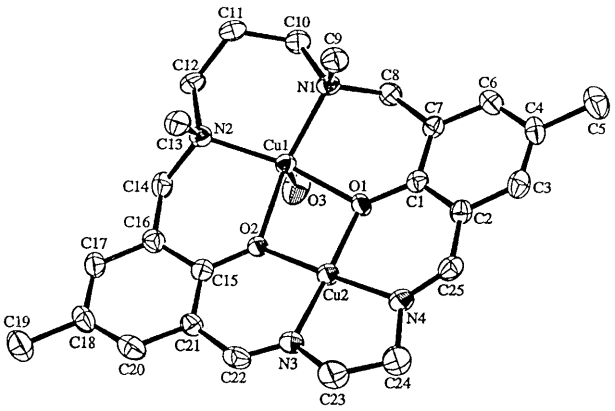

Fig. 2. An ORTEP view for $[Cu_2(L^1)(H_2O)](ClO_4)_2$·MeCN (**1**·$H_2O$·MeCN) with the atom numbering scheme.

Table 3. Selected Bond Distances and Angles for **1**·H_2O·MeCN

Bond Distances (Å)			
Cu(1)–O(1)	1.997(4)	Cu(1)–O(2)	2.005(3)
Cu(1)–O(3)	2.304(4)	Cu(1)–N(1)	2.012(4)
Cu(1)–N(2)	2.010(4)		
Cu(2)–O(1)	1.914(4)	Cu(2)–O(2)	1.898(4)
Cu(2)–N(3)	1.900(5)	Cu(2)–N(4)	1.902(5)
Cu(1)···Cu(2)	2.989(1)		
Bond Angles (°)			
O(1)–Cu(1)–O(2)	76.6(1)	O(1)–Cu(1)–O(3)	94.7(1)
O(1)–Cu(1)–N(1)	90.7(2)	O(1)–Cu(1)–N(2)	163.9(2)
O(2)–Cu(1)–O(3)	96.3(2)	O(2)–Cu(1)–N(1)	162.8(2)
O(2)–Cu(1)–N(2)	90.7(2)	O(3)–Cu(1)–N(1)	96.3(2)
O(3)–Cu(1)–N(2)	96.6(2)	N(1)–Cu(1)–N(2)	99.4(2)
O(1)–Cu(2)–O(2)	81.2(1)	O(1)–Cu(2)–N(3)	177.3(2)
O(1)–Cu(2)–N(4)	96.4(2)	O(2)–Cu(2)–N(3)	96.3(2)
O(2)–Cu(2)–N(4)	177.5(2)	N(3)–Cu(2)–N(4)	86.1(2)

The two methyl groups attached to the nitrogens are cis to each other. The water molecule at the axial site of Cu1 is situated trans to the *N*-methyl groups with respect to the mean molecular plane. The Cu1–Cu2 interatomic separation is 2.989(1) Å.

An ORTEP view for $[Cu_2(L^5)](ClO_4)_2$·2MeOH (**5**·2MeOH) is shown in Fig. 3 together with the atom numbering scheme. Relevant bond distances and angles are summarized in Table 4.

The crystal consists of the macrocycle $(L^5)^{2-}$ and two Cu^{II} ions; two perchlorate ions and two methanol molecules are free from coordination. The Cu1 in the aminic site assumes a nearly planar geometry with the Cu-to-donor bond distances of 1.968(6)–1.994(8) Å. The two methyl groups attached to the nitrogens N1 and N2 are situated cis to each other.

The geometry about Cu2 in the iminic site shows a large distortion to tetrahedron; the dihedral angle between the least-squares plane defined by Cu2, O1 and N4 and the least-squares plane defined by Cu2, O2 and N3 is 10.63°. The naphthalene ring is bent by 33.13 and 48.47° against the phenolic rings. This distortion about Cu2 arises from the steric repulsion between the hydrogen on C22 (C33) and that on C24 (C29). The Cu–Cu interatomic separation is 3.060(2) Å.

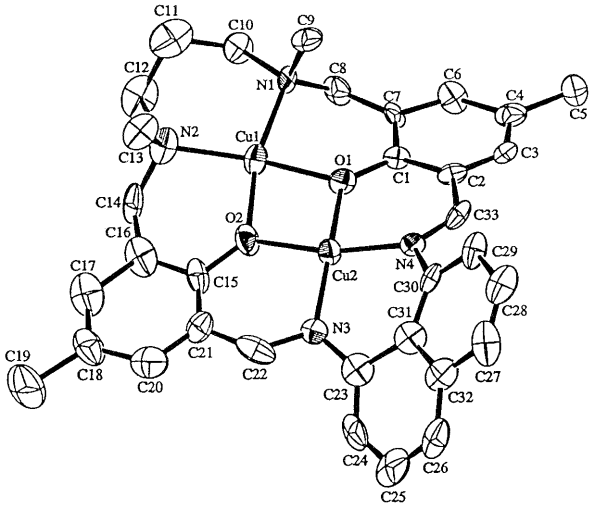

Fig. 3. An ORTEP view for $[Cu_2(L^5)](ClO_4)_2$·2MeOH (**5**·2MeOH) with the atom numbering scheme.

Table 4. Selected Bond Distances and Angles for **5**·2MeOH

Bond Distances (Å)			
Cu(1)–O(1)	1.980(6)	Cu(1)–O(2)	1.968(6)
Cu(1)–N(1)	1.994(7)	Cu(1)–N(2)	1.994(8)
Cu(2)–O(1)	1.937(6)	Cu(2)–O(2)	1.942(6)
Cu(2)–N(3)	1.933(7)	Cu(2)–N(4)	1.943(7)
Cu(1)···Cu(2)	3.060(2)		
Bond Angles (°)			
O(1)–Cu(1)–O(2)	75.4(2)	O(1)–Cu(1)–N(1)	92.7(3)
O(1)–Cu(1)–N(2)	165.0(3)	O(2)–Cu(1)–N(1)	163.1(3)
O(2)–Cu(1)–N(2)	90.1(3)	N(1)–Cu(1)–N(2)	100.7(3)
O(1)–Cu(2)–O(2)	76.9(2)	O(1)–Cu(2)–N(3)	168.4(3)
O(1)–Cu(2)–N(4)	96.5(3)	O(2)–Cu(2)–N(3)	93.0(3)
O(2)–Cu(2)–N(4)	167.9(3)	N(3)–Cu(2)–N(4)	94.4(3)

Physicochemical Properties. Complexes **1**–**5** each has a subnormal magnetic moment at room temperature. The μ_{eff} vs. T curves for **1** in the temperature range of 78–300 K are given in Fig. 4(A). The magnetic moment per Cu is 0.85 μ_B at room temperature and the moment decreased with decreasing temperature to 0.25 μ_B at liquid nitrogen temperature. The result indicates the operation of antiferromagnetic interaction within the molecule.

The cryomagnetic property of **1** was simulated by means of Bleaney–Bowers equation,[18]

$$\chi_A = (1-\rho)\{Ng^2\beta^2/kT\}[\exp(-2J/kT)+3]^{-1} + \rho\{Ng^2\beta^2/4kT\} + N\alpha \quad (1)$$

where ρ is the fraction of monomeric Cu^{II} impurity and other symbols have their usual meanings. A good simulation was obtained using the magnetic parameters $J = -310$ cm^{-1}, $g = 2.05$, $N\alpha = 70 \times 10^{-6}$ cm^3 mol^{-1} and $\rho = 0.015$, as indicated by the solid curve (A) in Fig. 4. The trace (B) is the best-fit for

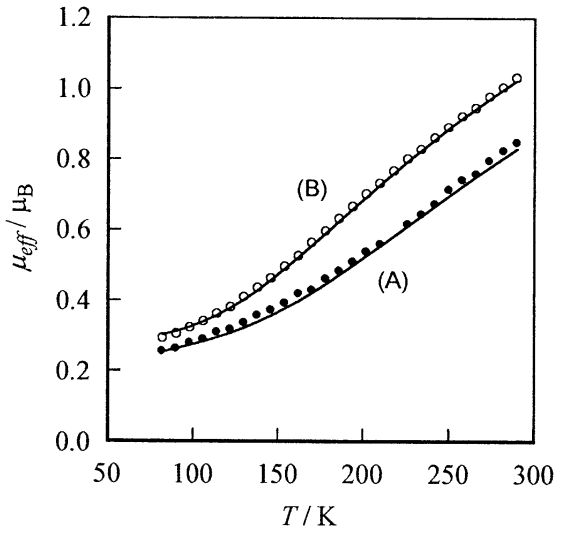

Fig. 4. Temperature-dependences of magnetic moment for (A) $[Cu_2(L^1)](ClO_4)_2$ (**1**) and (B) $[Cu_2(L)](ClO_4)_2$.

$[Cu_2(L)](ClO_4)_2$ using the parameters of $J = -252$ cm^{-1}, $g = 2.10$, $N\alpha = 60 \times 10^{-6}$ cm^3 mol^{-1} and $\rho = 0.015$.

Similarly, the cyomagnetic properties of **2**–**5** can be reproduced by the Bleaney-Bowers equation using the magnetic parameters: $J = -270$ cm^{-1}, $g = 2.10$, $N\alpha = 60 \times 10^{-6}$ cm^3 mol^{-1} and $\rho = 0.050$ for **2**, $J = -354$ cm^{-1}, $g = 2.10$, $N\alpha = 60 \times 10^{-6}$ cm^3 mol^{-1} and $\rho = 0.005$ for **3**, $J = -337$ cm^{-1}, $g = 2.10$, $N\alpha = 60 \times 10^{-6}$ cm^3 mol^{-1} and $\rho = 0.014$ for **4**, and $J = -340$ cm^{-1}, $g = 2.05$, $N\alpha = 100 \times 10^{-6}$ cm^3 mol^{-1} and $\rho = 0.020$ for **5**. The results demonstrate a fairly strong antiferromagnetic interaction for **1**–**5** and for their precursor $[Cu_2(L)](ClO_4)_2$ as well.

Electronic spectra of **1**–**5** were measured in dmf in the range of 300–900 nm. The numerical data are given in the Experimental Section. Complexes **1**–**3** show an intense band around 346–348 nm attributable to the π-π* transition associated with the azomethine linkage.[19,20] The ultraviolet spectral feature of **4** is complicated because of the conjugation of the azomethine group with the *o*-phenylene bridge and the spectra show three absorption bands at 346, 375 and 402 nm. The π-π* transition band for **5** is seen at a longer wavelength (392 nm), probably due to the distortion of the azomethine linkage (see Fig. 3).

In the visible region, **1**–**5** generally show two absorption bands due to the two non-equivalent Cu^{II} ions: ca. 470 and 654 nm for **1**, 646 and ca. 730 nm for **3**, 560 and 656 nm for **4**, and 656 and ca. 680 nm for **5**. One exception is **2** that shows one absorption band centered around 642 nm. This must be a superposition of two bands at similar wavelengths. One absorption band near 650 nm, commonly observed **1**–**5**, can be ascribed to the Cu^{II} in the aminic site. Another band appearing at different wavelengths for **1**–**5** may arise from the Cu^{II} in the iminic site.[21] It is evident that the d–d band maximum for the Cu^{II} in the iminic site shifts to longer wavelength in the order: **1** (ca. 470 nm) < **2** (ca. 640 nm) < **3** (ca. 730 nm); **4** (560 nm) < **5** (ca. 680 nm). This is in accord with an increasing order in tetrahedral distortion about the metal.[21]

Electrochemical properties of **1**–**5** were studied by means of cyclic voltammetry. All the complexes show two reversible or quasi-reversible couples in negative potential (see Fig. 5). We have confirmed that the Cu^{II}M^{II} complexes (M = Mn, Co, Ni, Cu, Zn) with an analogous ligand (Scheme 1: X = Br, R = CH_3, L^a = ethylene and L^b = trimethylene) show the Cu^{II}/Cu^{I} process at the aminic site at –0.69 ± 0.10 V vs. Ag$^+$/Ag (in DMSO)[5b] whereas the corresponding M^{II}Cu^{II} complexes show the Cu^{II}/Cu^{I} process at the iminic site at lower potential (–0.96 ± 0.04 V vs. Ag$^+$/Ag, in DMSO).[5c] This means that the aminic site is more flexible than the iminic site and is adaptable to a geometrical change on going from Cu^{II} to Cu^{I}.[22] Thus, the first couple appearing at practically the same potential for **1**–**5** (–0.62 ± 0.05 V vs. Ag$^+$/Ag) is attributable to the Cu^{II}/Cu^{I} process in the aminic site and the second couple to the Cu^{II}/Cu^{I} process in the iminic site. The second reduction potential increases in the order: **1** (–1.25 V) < **2** (–1.06 V) < **3** (–0.91 V) and **4** (–1.14 V) < **5** (–0.98 V). The trends are in accord with an increasing tetrahedral distortion about the metal in the iminic site.[22]

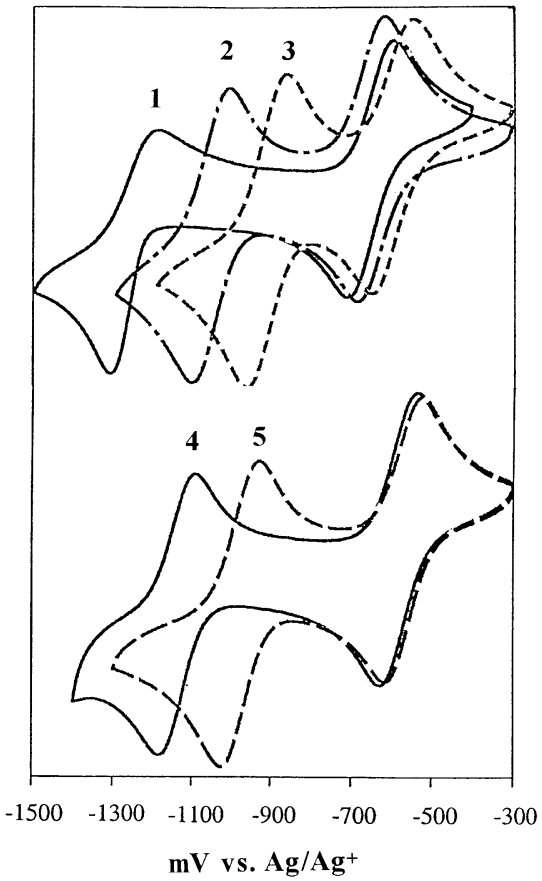

Fig. 5. Cyclic voltammograms of **1**–**5**. Conditions: in dmf solution containing TBAP (1×10^{-1} M), V vs. Ag/Ag$^+$ (TBAP/CH_3CN), scan rate 50 mV s^{-1}, glassy–carbon electrode, Pt counter electrode.

Macrocyclic Mononuculear Complexes. Preparation and General Characterization. For our object to develop heterodinuclear metal complexes using the macrocyclic ligands L^1–L^5, it is important to obtain mononuclear complexes that have a metal in either the aminic or iminic site. In this work

we attempted to convert the dinuclear complexes into mononuclear complexes by the demetallation of one Cu ion. Eventually we succeeded in obtaining [Cu(L^{i})]·xNaClO$_4$ by the treatment of **1**–**5** with Na_2S in acetonitrile: [Cu(L^1)]·0.8NaClO$_4$ (**1′**·0.8NaClO$_4$), [Cu(L^2)] (**2′**), [Cu(L^3)]·NaClO$_4$ (**3′**·NaClO$_4$), [Cu(L^4)] (**4′**) and [Cu(L^5)]·2.1NaClO$_4$ (**5′**·2.1NaClO$_4$). The IR spectra of **1′**·0.8NaClO$_4$ and **5′**·2.1NaClO$_4$ each has an intense band at 1100 cm^{-1} typical of NaClO$_4$.[23] Evidently, **1′** and **5′** are contaminated by NaClO$_4$. On the other hand, **3′**·NaClO$_4$ shows a split of the ν_3 perchlorate vibration into two (1095, 1063 cm^{-1}). Furthermore, the FAB mass spectrum of **3′**·NaClO$_4$ has a prominent ion peak at m/z 534.4 that corresponds to {NaCu(L^3)}$^+$. The results suggest that the Na^{I} is accommodated in the aminic site with the coordination of the perchlorate ion. This has been demonstrated by X-ray crystallographic studies as discussed later.

The visible spectrum of **2′** in dmf has a d–d maximum at 607 nm that is compared to that for *N*,*N*′-trimethylenedisalicylideneaminatocopper(II) (602 nm in nujol mull[21] and 605 nm in acetonitrile[24]). Similarly, the d-d band maximum of **4′** (590 nm) is compared to that for *N*,*N*′-o-phenylene-disalicylideneaminatocopper(II).[20] The spectral results for **2′** and **4′** add a support to the suggestion that the Cu exists in the iminic site in each complex. That is, the Cu in the aminic site is eliminated by the treatment with Na_2S.

Crystal Structures. The X-ray crystallographic studies have been made for [Cu(L^2)] (**2′**), [Cu(L^3)]·NaClO$_4$ (**3′**·NaClO$_4$) and [Cu(L^4)] (**4′**) to specify the site to which the Cu^{II} is bound. ORTEP drawings of **2′**, **3′**·NaClO$_4$ and **4′** are shown in Figs. 6, 7 and 8, respectively, and the selected bond distances and angles of the complexes are given in Tables 5, 6 and 7, respectively.

The X-ray crystallography for **2′** unambiguously demonstrates that the Cu^{II} in the aminic site is eliminated (Fig. 6). The Cu existing in the iminic site has a pseudo tetrahedral geometry; the dihedral angle between the least-squares plane defined by Cu, O1 and N2 and the plane defined by Cu, O1* and N2* is 32.17°. This distortion is compared to that found for analogous [Cu(L$^{2;3}$)] (dihedral angle: 35.56°).[6] The two methyl groups at-

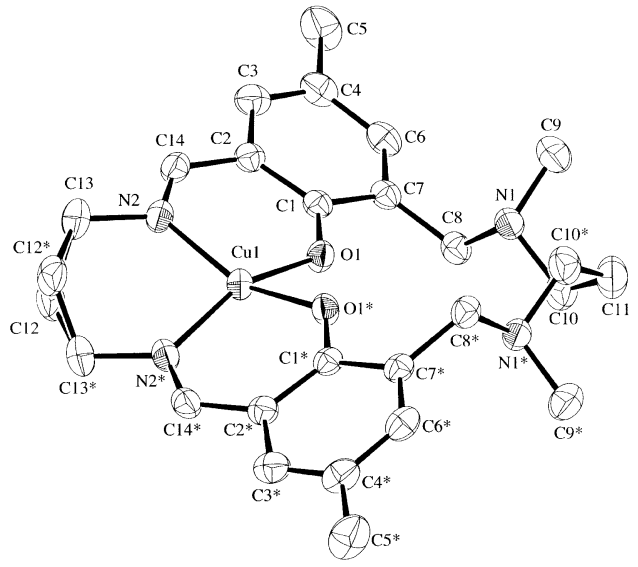

Fig. 6. An ORTEP view for [Cu(L^2)] (**2′**) with the atom numbering scheme.

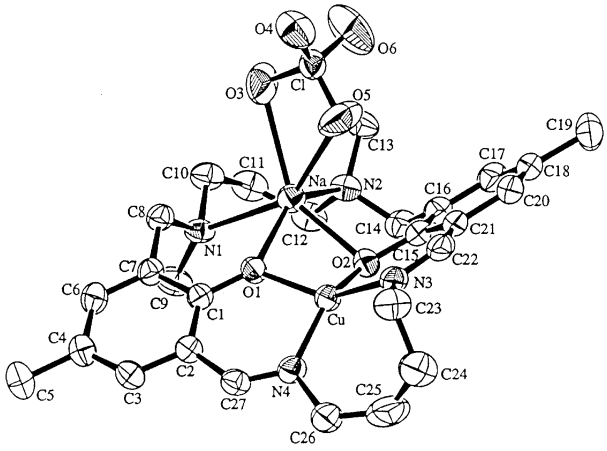

Fig. 7. An ORTEP view for [Cu(L^3)]·NaClO$_4$ (**3′**) with the atom numbering scheme.

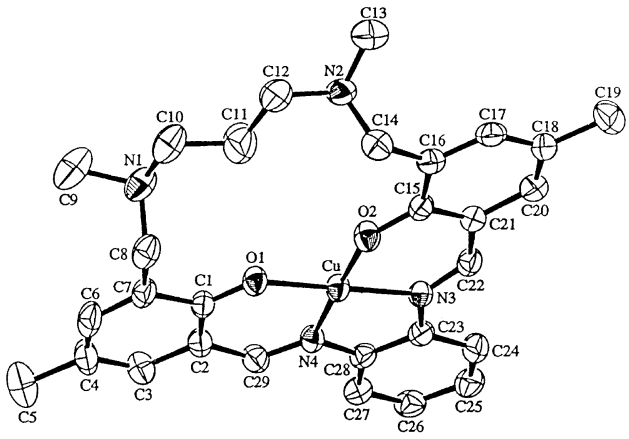

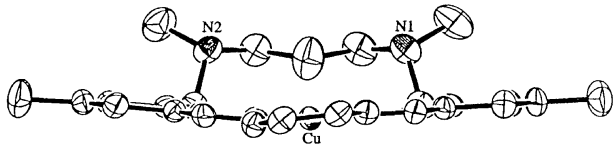

Fig. 8. An ORTEP view for [Cu(L^4)] (**4′**) with the atom numbering scheme.

Table 5. Selected Bond Distances and Angels for **2′**

Bond Distances (Å)			
Cu–O(1)	1.906(2)	Cu–N(2)	1.960(3)
Bond Angels (°)			
O(1)–Cu–O(1)[a)]	86.1(1)	O(1)–Cu–N(2)	93.0(1)
O(1)–Cu–N(2)[a)]	156.1(1)	N(1)–Cu–N(2)[a)]	97.2(2)

a) Symmetry operation (2-x, y, 3/2-z).

Table 6. Selected Bond Distances and Angles for **3′**·$NaClO_4$

Bond Distances (Å)			
Cu–O(1)	1.920(2)	Cu–O(2)	1.893(3)
Cu–N(3)	1.949(3)	Cu–N(4)	1.962(3)
Na–O(1)	2.270(3)	Na–O(2)	2.296(3)
Na–O(3)	2.615(4)	Na–O(5)	2.575(4)
Na–N(1)	2.548(3)	Na–N(2)	2.405(4)
Cu(1)···Na	3.040(2)		
Bond Angles (°)			
O(1)–Cu–O(2)	87.8(1)	O(1)–Cu–N(3)	146.3(1)
O(1)–Cu–N(4)	93.8(1)	O(2)–Cu–N(3)	93.4(1)
O(2)–Cu–N(4)	148.7(1)	N(3)–Cu–N(4)	102.0(1)

Table 7. Selected Bond Distances and Angles for **4′**

Bond Distances (Å)			
Cu–O(1)	l.901(3)	Cu–O(2)	1.915(3)
Cu–N(3)	l.955(3)	Cu–N(4)	1.948(3)
Bond Angles (°)			
O(1)–Cu–O(2)	89.4(1)	O(1)–Cu–N(3)	176.2(1)
O(1)–Cu–N(4)	93.5(1)	O(2)–Cu–N(3)	93.5(1)
O(2)–Cu–N(4)	176.6(1)	N(3)–Cu–N(4)	83.5(1)

tached to the nitrogens are situated trans to each other with respect to the mean $N(amine)_2O_2$ plane. The trimethylene chain combining the imino nitrogens (N2 and N2*) adopts a deformed conformation. Such conformational features in the vacant aminic site may arise from a strain within the macrocyclic framework.

The X-ray crystallography for **3′**·$NaClO_4$ demonstrates that the Cu in the aminic site is eliminated and the Na^I ion is accommodated in this site (Fig. 7). The Na^I has a distorted six-coordinate environment together with a chelating perchlorate group. The Na-to-donor bond distances range from 2.270(3) to 2.615(4) Å. The two methyl groups attached to the amine nitrogens are situated trans to each other with respect to the mean $N(amine)_2O_2$ plane. The geometry about the Cu in the iminic site is significantly distorted to tetrahedron: the dihedral angle between the plane defined by Cu, O1 and N4 and the plane defined by Cu, O2 and N3 is 43.80°. The Cu–Na interatomic distance is 3.040(2) Å. It appears that the aminic site of **3′** has a flexibility for accommodating Na^I owing to the elongation in the lateral chain in the iminic site.

An ORTEP view of **4′** again demonstrates the selective elimination of the Cu from the aminic site. The Cu^{II} bound to the iminic site has an essentially planar geometry. The Cu-to-donor bond distances range from 1.901(3) to 1.955(3) Å. The vacant aminic site is expanded so as to reduce a strain within the macrocyclic framework. The molecule except for the –(Me)N–$(CH_2)_3$–N(Me)– part in the aminic site forms a good coplanarity (see the edge view in Fig. 8).

Conclusion. The [1:1] condensation of the dinuclear Cu^{II} complex of the acyclic prolig and, *N*,*N*′-dimethyl-*N*,*N*′-trimethylenedi(5-methyl-3-formyl-2-hydroxybenzylamine, with an aliphatic or aromatic diamine affords the dinuclear Cu^{II} complexes of the macrocyclic ligands (L^1–L^5), $[Cu_2(L^i)](ClO_4)_2$ ($L^i = L^1$ with ethylenediamine) (**1**), L^2 with trimethylenediamine (**2**), L^3 with tetramethylenediamine (**3**), L^4 with *o*-phenylenediamine (**4**) and L^5 with 1,8-naphthalenediamine (**5**)). The two Cu^{II} ions are bound to the $N(amine)_2O_2$ and $N(imine)_2O_2$ sites of each macrocycle, bridged by the two phenolic oxygens. A strong antiferromagnetic interaction occurs between the two metal ions. The d–d band maximum of the Cu in the iminic site shifts in the order: **1** (ca. 470 nm) < **2** (ca. 640 nm) < **3** (ca. 730 nm) and **4** (560 nm) < **5** (ca. 680 nm). Similarly, the Cu^{II}/Cu^I reduction potential due to the Cu in the iminic site shifts in the order: **1** (–1.25 V) < **2** (–1.06 V) < **3** (–0.91 V) and **4** (–1.14 V) < **5** (–0.98 V). The trends are in accord with an increasing order in tetrahedral distortion about the metal. The d–d band maximum and the Cu^{II}/Cu^I reduction potential of the Cu^{II} in the aminic site were invariant among the complexes.

The dinuclear complexes were converted into mononuclear complexes, $[Cu(L^i)]\cdot x NaClO_4$, when treated with Na_2S in acetonitrile. The selective demetallation of the Cu^{II} in the aminic site is demonstrated based on X-ray crystallographic studies. The mononuclear Cu^{II} complexes can be precursors for heterodinuclear $Cu^{II}M^{II}$ complexes. Studies in this line are under way in our laboratory.

This work was supported by Scientific Research on Priority Area "Metal-assembled Complexes" (No. 10149106) and an International Scientific Research Program (No. 09044093) from the Ministry of Education, Science and Culture. The authors thank Mr. Naoki Usuki and Mr. Keisuke Arimura in our laboratory for their help in magnetic analyses.

References

1 D. E. Fenton and H. Ōkawa, *Chem. Ber.*, **130**, 433 (1997).

2 H. Ōkawa, H. Furutachi, and D. E. Fenton, *Coord. Chem. Rev.*, **174**, 51 (1998).

3 C. Fraser, L. Johnson, A. L. Rheingold, B. S. Haggerty, G. K. Williams, J. Whelan, and B. Bosnich, *Inorg. Chem.*, **31**, 1835 (1992); D. G. McCollum, G. P. A. Yap, A. L. Rheingold, and B. Bosnich, *J. Am. Chem. Soc.*, **111**, 1365 (1996) and references therein.

4 M. Yonemura, Y. Matsumura, M. Ohba, H. Ōkawa, and D. E. Fenton, *Chem. Lett.*, **1996**, 601.

5 a) M. Yonemura, Y. Matsumura, H. Furutachi, M. Ohba, H. Ōkawa, and D. E. Fenton, *Inorg. Chem.*, **36**, 2711 (1997). b) M. Yonemura, M. Ohba, K. Takahashi, H. Ōkawa and D. E. Fenton, *Inorg. Chim. Acta*, **283**, 72 (1998). c) M. Yonemura, Y. Nakamura, N. Usuki, and H. Ōkawa, *Proc. Ind. Acad. Sci.*, **112**, 291 (2000). d) M. Yonemura, N. Usuki, Y. Nakamura, M. Ohba, and H. Ōkawa, *J. Chem. Soc., Dalton Trans.*, **2000**, 3624.

6 S. Karunakaran and M. Kandaswamy, *J. Chem. Soc., Dalton Trans.*, **1994**, 1595.

7 N. F. Curtis, *J. Chem. Soc.*, **1961**, 3147.

8 E. A. Boudreaux and L. N. Mulay, "Theory and Applications of Molecular Magnetism," Wiley (1976), p. 491.

9 J. C. Duff, *J. Chem. Soc.*, **1941**, 547.

10 G. Lock, *Chem. Ber.*, **63**, 551 (1930).

11 D. T. Cromer and J. T. Waber, "International Tables for X-ray Crystallography, Vol. IV, Kynoch Press," Birmigham (1974).

12 D. C. Creagh and W. J. McAuley, "International Tables for

X-ray Crystallography," ed. by A. J. C. Wilson et al., Kluwer Acad. Pub., Boston (1992), pp. 219–222.

13 D. C. Creagh and H. H. Hubbell, "International Tables for X-ray Crystallography," ed. by A. J. C. Wilson et al., Kluwer Acad. Pub., Boston (1992), pp. 200–206.

14 TEXSAN, Molecular Structure Corporation, Houston, TX, 1985.

15 C. K. Johnson, Report 3794, Oak Ridge National Laboratory, Oak Ridge, TN (1965).

16 M. Tanaka, H. Ōkawa, I. Hanaoka, and S. Kida, *Chem. Lett.*, **1974**, 71.

17 K. Nakamoto, "Infrared Spectra of Inorganic and Coordination Compounds, 2nd Ed.," Wiley, New York (1963), pp. 175–176.

18 B. Bleaney and K. D. Bowers, *Proc. R. Soc. London, A*, **214**, 451 (1952).

19 B. Bosnich, *J. Am. Chem. Soc*, **90**, 627 (1968).

20 R. S. Downing and F. L. Urbach, *J. Am. Chem. Soc.*, **91**, 5977 (1969).

21 S. J. Gruber, C. M. Harris, and E. Sinn, *J. Inorg. Nucl. Chem.*, **30**, 1805 (1968).

22 G. S. Patterson and R. H. Holm, *Bioinorg. Chem.*, **4**, 257 (1974).

23 F. A. Miller and C. H. Wilkins, *Anal. Chem.*, **24**, 1253 (1952).

24 B. Xiong, B. Song, J. Zuo, X. You, and X. Huang, *Polyhedron*, **15**, 903 (1995).